

Keywords: crumple zone; lumped mass model; head performance criterion; neck injury criteria

**Vaidas LUKOŠEVIČIUS, Robertas KERŠYS*, Artūras KERŠYS,
Rolandas MAKARAS, Janina JABLONSKYTĖ**

Kaunas University of Technology, Transport Engineering Department
Studentų st. 56, Kaunas, LT-43124, Lithuania

*Corresponding author. E-mail: robertas.kersys@ktu.lt

THREE- AND FOUR-MASS MODELS FOR VEHICLE FRONT CRUMPLE ZONE

Summary. The article deals with the applicability of the three- and four-mass crumple zone models by optimization of the vehicle front crumple zone in case of a collision. The possibilities for integrating the requirements for individual crumple zones are discussed. The crumple model for special crumple zone elements has been proposed. Optimum parameter limits for the deformable elements have been identified, and complex influence of the damping elements used has been demonstrated. The need for adjustment of the optimization process for different vehicle load has been identified. The article analyzes the requirements applicable to the front crumple zone of a light passenger vehicle in case of a front collision by employing simple models.

1. INTRODUCTION

In the design process of a vehicle body, safety requirements are considered with particular care. In addition to the strength and durability requirements, the supporting structures are to meet special requirements, such as maintaining the safety spaces of specific dimensions and shape in the passenger compartment or cabin enabling the driver and passengers to survive during an accident. Hence, safety requirements may become central not only for designing the vehicle body structures but also for selecting the configuration of the entire vehicle. The space occupied by people needs to be surrounded with a rigid and strong frame, including crumple zones, which protect the occupants against overloads by absorbing the impact energy.

The supporting structures should be not only strong enough but also deformable in a way that provides protection of the driver and passengers against overloads by absorbing the energy. Owing to specificity of the requirements, specially structured elements are often used or a crumple zone is formed using basic elements of the supporting structure. The most accurate requirements available at present are the ones that apply to the case where the kinetic energy of the entire vehicle needs to be damped, i.e. in the case of a front collision or impact into a solid obstacle. The major focus is usually on the front crumple zone owing to the majority of traffic accidents being the collisions or impacts into an obstacle. Moreover, the traffic accidents usually take place at higher speeds.

2. REQUIREMENTS TO A VEHICLE IN CASE OF A FRONT COLLISION

The Europe United Nations Economic Commission establishing key vehicle structure specifications defines safety requirements applicable to vehicle bodies. The EU has passed a series of dedicated directives defining key limit parameters for securing human life and health. As noted in Directive 96/79/EC [1-4], the maximum head deceleration during an impact is not to exceed 80 g ($g = 9.81 \text{ m/s}^2$) with the maximum permissible exposure duration of 3 ms.

One of the key parameters in securing human life and health is the *HPC* (Head Performance Criterion). All vehicle safety tests involving an occupant are adjusted for this permissible overload. It is calculated using the following expression:

$$HPC = (t_1 - t_2) \left[\frac{1}{t_2 - t_1} \int_{t_1}^{t_2} a(t) dt \right]^{2.5} \quad (1)$$

where a – acceleration, m/s^2 , and $t_2 - t_1$, – time interval selected, s . Time t_1 and t_2 are selected for the highest *HPC*. ($t_2 - t_1$) should be within 3 — 36 ms. The *HPC* is not to exceed 1000 [4].

Another important human body part is the neck. Neck injury is defined by the *NIC* (Neck Injury Criteria) consisting of the *NTC* (Neck Tension Criterion) and *NSC* (Neck Shear Criterion) criteria, which define the loads developing due to the head inertia [5]. In case of a rebound (rear impact), the impact is compensated by the head support fit inside the backrest. This is an autonomous system in contemporary vehicles, which limits the backward bending of the neck. The maximum permissible neck tension force is 3.5 kN and shear force is 3.1 kN. Moreover, the maximum forces at the respective moment of time shall meet the following conditions:

For the *NTC*:

$$\begin{cases} F \leq 3.3 - 11.428 \cdot 10^{-3} t, & \text{where } 0 \leq t \leq 35; \\ F \leq 5.4 - 71.667 \cdot 10^{-3} t, & \text{where } 35 \leq t \leq 60; \\ F \leq 1.1 t, & \text{where } t \geq 60; \end{cases} \quad (2)$$

For the *NSC*:

$$\begin{cases} F \leq 3.1 - 64 \cdot 10^{-3} t, & \text{where } 35 \leq t \leq 25; \\ F \leq 1.5 t, & \text{where } 25 \leq t \leq 35; \\ F \leq 3.1 - 44.444 \cdot 10^{-3} t, & \text{where } 35 \leq t \leq 45; \\ F \leq 1.1 t, & \text{where } t \geq 45; \end{cases} \quad (3)$$

where F – force acting on the neck, Kn, and t – duration of exposure to the force, ms. Thoracic cell-related requirements have been established as well. The force acting on the chest during the impact into the steering wheel shall not exceed 11.5 kN. The maximum force of 11.1 kN is recommended for the steering wheel. The maximum possible displacement of the chest center point [2-5] is 325 mm, and the maximum chest deceleration acting for up to 3 ms shall not exceed 60 g. The recommended effective occupant's displacement from the backrest is 300 mm. The residual space for legs is 250 mm. These values are mandatory to secure occupant's survival and are followed in development of the safety belt requirements. The maximum restraining force shall not exceed 15 kN. Belt energy damping coefficient (k) should be 0.8. The amount of the energy absorbed shall be 2.6 - 4.95 kJ. The recommended belt breaking force shall not exceed 22 kN ($v = 50$ km/h). These requirements reflect the key design criteria for vehicle body crumple zones but are not the only requirements to be met. An additional requirement has been established to the front crumple zone or its element – the bumper, namely, the functionality of the vehicle units shall not be impaired in case of a collision at a low speed (up to 8 km/h). The most sensitive units in this respect are the vehicle lighting devices. To avoid any damage to the filament bulb (i.e. rupture of its filaments), deceleration shall not exceed 4 g [2-5]. The objective of optimization in terms of splitting the vehicle into crumple zones and optimization of the crumple zones is to make sure that the aforementioned requirements are met at the maximum possible initial impact speed of the vehicle. Splitting into zones is also relevant to insurance companies. Standard front collision test is conducted at 64 km/h speed [6-9].

3. DYNAMIC THREE – MASS MODEL

Following the analysis of several applicable vehicle models [10-14], the three-mass model presented in Fig. 1 has been found to be the simplest option, which still reflects the key deformation characteristics.

Here, the crumple zone is split into three sections:

1. Bumper zone (m_1), i.e., zone 1, covers the space from the beginning of the bumper to the radiator.

2. Engine zone (m_2), i.e., zone 2, covers the space from the radiator to the engine. The possibility of flattening of the radiator is taken into account in calculation of the deformation.
3. Vehicle body zone (m_3), i.e., zone 3, covers the space between the engine and the front wall of the passenger compartment.

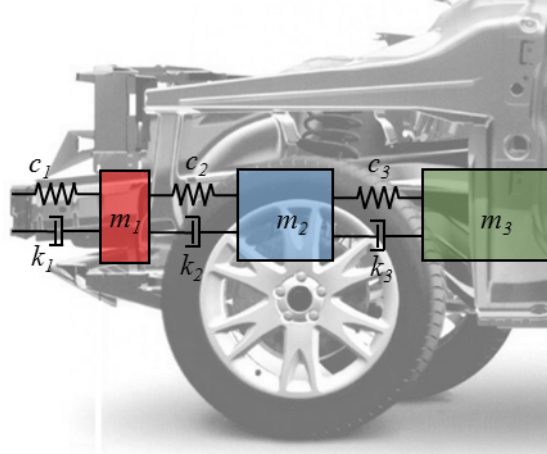


Fig. 1. Three-mass model for the front crumple zone

Splitting of the model into three masses is relative. Each part reflects a specific zone which includes the units located within it. For example, the following units are attributed to the engine zone besides the engine: the radiator, front part of the side member up to the engine, etc. The splitting has been performed intentionally. Irrespective of the impact process, the sequence of deformation and energy absorption could be observed, i.e., deformation of the units located further from the bumper starts only after the deformation of the preceding units has ended. Moreover, each zone has its main stiffness and damping elements. This functional completeness of the zone means that it can be considered as an individual mass in the vehicle configuration. The tests involving splitting of the crumple zone into fewer or more zones were not effective. With fewer zones, all of the aforementioned requirements were impossible to meet, whereas in case of a larger number of the zones, the requirements to individual zones became unspecific.

The three-mass model reflects the key masses involved in the impact and provides the picture of the modern trend in impact research, namely, the objective to make the level of damages to the vehicle body dependent on the initial impact speed. The model is described using a system of equations (4).

$$\begin{cases} m_1\ddot{x}_1 + k_1\dot{x}_1 + c_1x_1 + k_2(\dot{x}_1 - \dot{x}_2) + c_2(x_1 - x_2) = 0; \\ m_2\ddot{x}_2 + k_2(\dot{x}_2 - \dot{x}_1) + c_2(x_2 - x_1) + k_3(\dot{x}_2 - \dot{x}_3) + c_3(x_2 - x_3) = 0; \\ m_3\ddot{x}_3 + k_3(\dot{x}_3 - \dot{x}_2) + c_3(x_3 - x_2) = 0; \end{cases} \quad (4)$$

The system of equations has been calculated under the modified Runge-Kutta method. The uncertainty develops in the calculations because of the values of the impact damping coefficient. Although the theoretical model provides fairly clear values of the damping coefficient, absolutely accurate assessment of the damping is impossible in calculations of a specific vehicle owing to the structural complexity. Additional issues occur owing to the natural wear of the vehicle. City car and sedan have been selected for the calculations. Calculations at the first stage did not account for the damping. The mass and stiffness data are provided in Table 1.

At first, front impact of city car running at 2.22 m/s (8 km/h) is analyzed. At this speed, the bumper fully absorbs the impact energy but is not subject to any plastic deformations. The results are presented in Fig. 2 - 4. The displacement graph (Fig. 2) suggests that the largest displacements have been registered in the bumper zone. The resulting maximum displacement for the bumper zone is 94 mm, engine zone – 81 mm, and vehicle body zone – 47 mm.

The bumper displacement suggests that, at this speed, the bumper is not deformed completely yet, as its complete deformation is 125 mm. This degree of displacement does not cause any particular issues in the vehicles manufactured in the U.S. owing to larger bumper zones. The resulting displacement, however, is fairly large and difficult to sustain for the vehicles manufactured in Europe.

Hence, at the initial speed of 8 km/h, the aforementioned requirements regarding preservation of functioning of the electrical system cannot be met.

Table 1

Calculation data

Zone characteristics		Data		
		City car	Sedan	Numerical model
1	Mass m_1 , kg	15	18	15
	Stiffness c_1 , kN/m	453	580	350 - 450
	Damping k_1 , kNs/m	2.5	3.2	0.52 - 2.6
	Limit deformation, m	0.125	0.125	0.125
	Limit load, kN	56.9	73	40 - 60
2	Mass m_1 , kg	100	120	275
	Stiffness c_1 , kN/m	1000	3500	1000 - 1400
	Damping k_1 , kNs/m	6.6	13.3	2.36 - 11.38
	Limit deformation, m	0.38	0.31	0.38
	Limit load, kN	452.3	710	290 - 500
3	Mass m_1 , kg	1250	1645	655
	Stiffness c_1 , kN/m	4000	2420	2000 - 4050
	Damping k_1 , kNs/m	15.3	18.9	15.3 - 76
	Limit deformation, m	0.25	0.41	0.25
	Limit load, kN	607	870	400 - 610

Deceleration is one of the major parameters during a collision. Deceleration values for the zone are presented in Fig. 3. The resulting deceleration values for the vehicle body zone are considerably lower than those for the bumper zone. During the analysis of the impact process, the highest deceleration values for the bumper zone have been found to have a fairly limited effect on the occupant. Deceleration requires better control only starting with zone 2 in order to reduce the effect on the occupant.

The most hazardous deceleration is deceleration of the vehicle body zone. The values, however, are low in this case. At the initial impact speed of 8 km/h, deceleration for the bumper zone is 26.4 g, engine zone – 7.1 g, and vehicle body zone – 5.2 g. The identified values are not absolutely life-threatening. The deceleration analysis has suggested that the effect of damping is one of the major issues when dealing with the tasks related to impact. The effect of damping on deceleration is shown in Fig. 4. Light and non-rigid bumper is subject to strong vibrations where damping is absent.

The highest deceleration values for the larger part of the impact are considerably higher than in case of sufficient damping of the bumper. Heavier units are subject to lower vibrations (Fig. 5). Deceleration of these zones, however, has stronger effect on the occupant. The damping coefficient not only eliminates the resulting sweeps but also reduces their maximum values. The analysis of the experiment data, namely, the nature of the vibrations registered during the tests, suggests that certain vehicle body elements, such as its plastic parts, and noise damping facilities act as vibration damping elements, and the elements of the designed crumple zones cannot be modelled as being absolutely elastic. The damping coefficient values used in the model have been selected experimentally, according to Afanasyev et al [3]. The main requirement applicable to bumper zone design is not exceeding the deceleration value of 4 g acting on the vehicle body (lighting system) at the impact speed of 8 km/h.

According to the U.S. standards, in case of a head-on collision at the speed of 5 miles/h (8 km/h), the vehicle should not have any damages, and the impact shall be absorbed at the span of 5 – 8 cm [3]. Although deceleration depends on the stiffness, the bumper shall be provided with the stiffness value, which helps to meet the aforementioned condition. Fig. 6 presents the data showing the dependence of deceleration of zone 2 (engine zone) fitted with vehicle lighting system devices on the bumper stiffness. As suggested by the graph, at the impact speed of 8 km/h, the required deceleration value is reached at 450 kN/m stiffness. It is difficult to meet this condition in case of the European vehicles

owing to the smaller dimensions. Hence, the initial impact speed is reduced to 5 km/h, and the requirements of absence of any damages no longer applies, i.e. plastic deformations of the bumper are tolerated. This enables using bumpers of simpler structure. To meet the conditions, the bumper needs stiffening by reduction of its deformation.

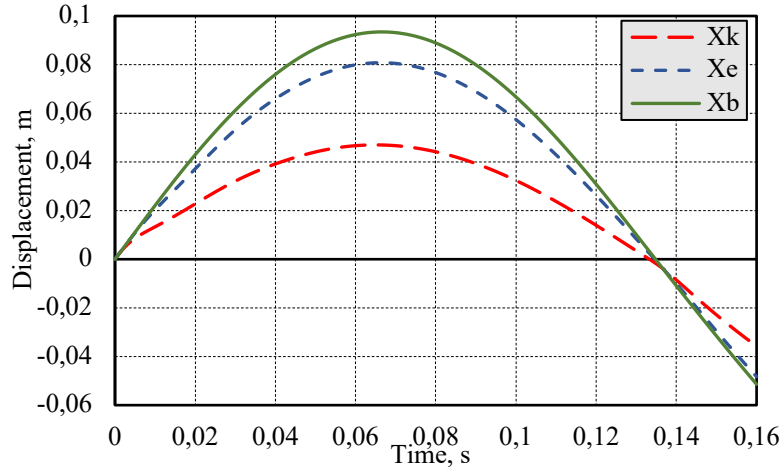


Fig. 2. Displacement of the units in the front crumple zone at the initial speed of 8 km/h, where Xb – bumper displacement, Xe – engine zone displacement, and Xk – vehicle body displacement

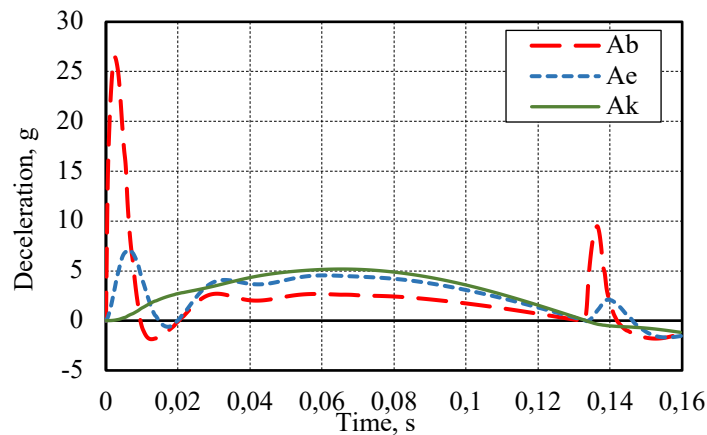


Fig. 3. Deceleration values for the units in the front crumple zone with the vehicle running at the initial impact speed of 8 km/h, where Ab – bumper deceleration, Ae – engine zone deceleration, and Ak – vehicle body deceleration

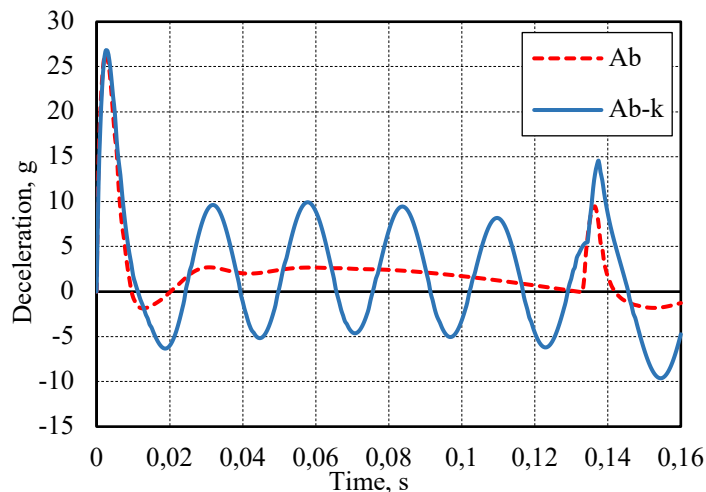


Fig. 4. Bumper deceleration with (Ab) energy damping, $k = 2.5$ kNs/m, and without energy damping (Ab-k)

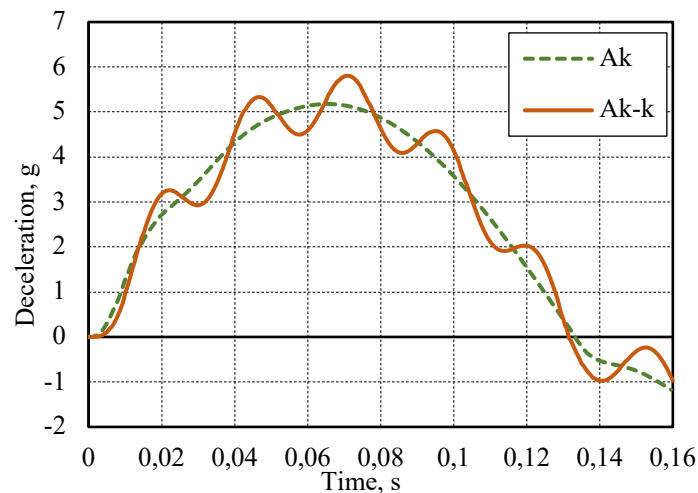


Fig. 5. Vehicle body deceleration with (Ak) and without (Ak-k) energy damping

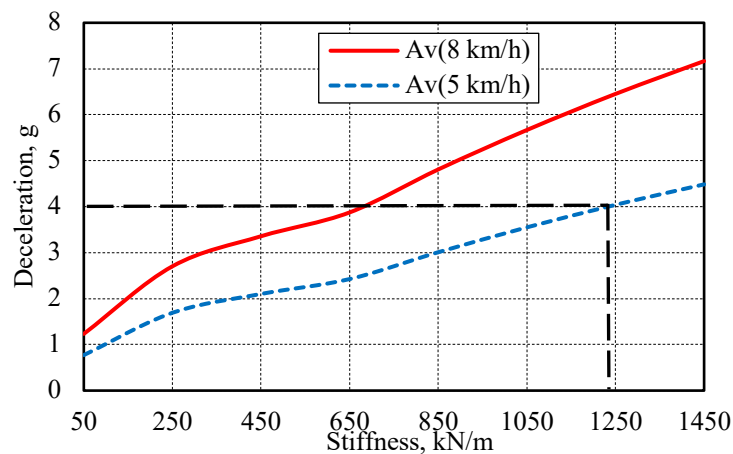


Fig. 6. Dependence of deceleration of zone 2 on bumper stiffness

To reach 4 g deceleration at the impact speed of 5 km/h, stiffness would have to be increased to 1250 kN/m (Fig. 6). Bumpers meeting this criterion were used several decades ago, when energy absorption facilities were not in place. In the case analyzed, the second condition must be met, i.e. maximum deformation of the bumper shall not exceed 0.125 m. Fig. 7 presents the dependence of displacement on the bumper stiffness. As suggested by the data presented, at 8 km/h speed, the 0.125 m limit is exceeded at 250 kN/m, whereas at 5 km/h, the limit is exceeded at the stiffness of 150 kN/m.

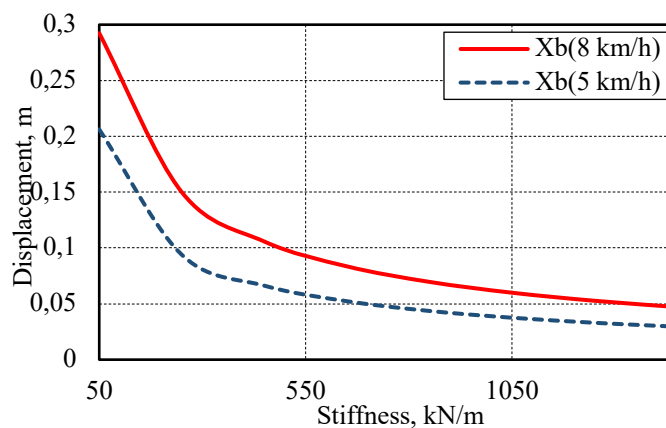


Fig. 7. Dependence of bumper displacement on bumper stiffness

The dependences presented in Fig. 6 and 7 suggest that satisfying the bumper safety condition at 8 km/h requires providing the bumper stiffness of 250 – 450 kN/m. At 5 km/h, the limits are much broader. In view of the both conditions, finding appropriate bumper stiffness does not require any particular efforts. The selection possibilities at this stage are limited only by the potential bumper deformations. The three-mass model has enabled identifying the key weaknesses of the simulation. The major weakness is that the deformation properties of a zone are impossible to describe using linear stiffness elements at higher speeds. These elements are appropriate only until plastic deformations have started, for example, in case of an American version of the bumper zone. In case of a European version of the zone, certain plastic deformation model must be taken into account. In the present work, it is assumed that the elements of the main crumple zone are designed for continued plastic deformation, i.e. the elements shall not lose their stability after plastic deformation has started, and the deformed element develops fine axial waves which are then subject to flattening [15]. Hence, in this work, the conditional deformation model presented in Fig. 8 has been selected for the elements. At the initial moment (OA), under the action of load F , stiffness varies linearly up to the limit deformation AB established for each zone. This limit deformation is achieved at the respective limit load F_r .

$$c = c_0 + (c_d - c_0) \frac{x_d}{x_r} \quad (5)$$

where x_d – plastic deformation and x_r – limit displacement.

Next stage (AB) is plastic deformation. As soon as the load has exceeded limit value Δi (after the element has been flattened), stiffness increases by ten (BD). The elastic deformation module in the plastic zone increases in a linear mode according to the plastic deformation value: from the initial to the value selected for the element subject to full plastic deformation.

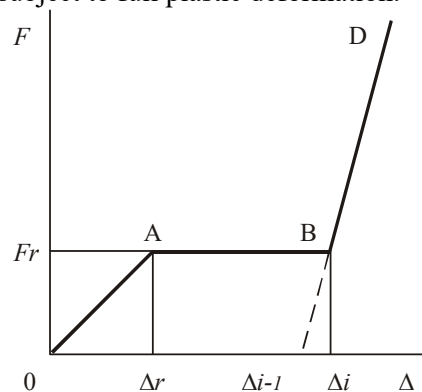


Fig. 8. Dependence of stiffness on load

Another property of the three-mass model which presents considerable limitation to its application is that deformation values of the zones located after the bumper need to be aligned with the maximum permissible deformation values for the occupant. Hence, a more complex four-mass dynamic model is required for further calculations.

4. DYNAMIC FOUR – MASS MODEL

In the four-mass dynamic model, an attempt has been made to assess the effect of occupant's behavior and occupant's safety systems. This is relevant for the analysis involving human's critical effects, as it includes assessment (and adjustment) of the characteristics of the seat belt and backrest. Seat belts are the safety means for occupant's movement forward. The belt material is selected specifically to provide respective elasticity as well as damping properties [16]. Moreover, the impact specifics, which is clearly evident in the three-mass model as well, needs to be taken into account. The impact force is usually stronger than the vehicle structure is capable of absorbing at the initial moment. This causes rebound of the vehicle. The rebound depends on the properties of the elements, which absorb the energy, and on the initial speed. The rebound acceleration is lower than the vehicle

post-impact deceleration, but this is very hazardous to the occupant, as the occupant is thrown back. This is taken into account during backrest design process. Backrests are intended not only to hold the human back but also to damp the impact in order to prevent injuries. Neck is the weakest point, which is very sensitive to the rebound acceleration. Headrests are fitted to the backrests specifically to protect the neck, and although headrests perform the same functions as the backrests, the former shall enable greater displacements and provide more effective energy absorption, as the speed of the head is higher than that of the chest during the rebound. Hence, the backrest is considered to be an individual safety element with its own characteristics c_5 and k_5 . All these elements enable more accurate assessment of the links to the vehicle body. The four-mass model used is presented in Fig. 9. Human mass is assumed to be 75 kg in the model calculations. The use of several occupants (masses) is also possible in the calculations. In this case, the masses are summed up, and general safety systems apply to all the occupants.

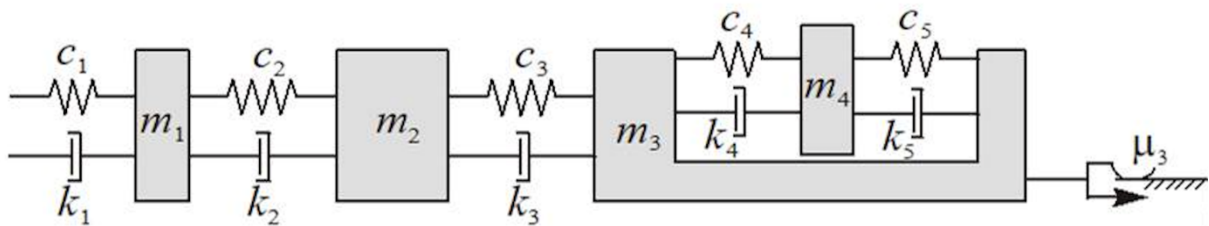


Fig. 9. Four-mass model for the front crumple zone

As soon as the calculation of greater impact speeds had started, the vehicle was noticed to rebound to an unrealistically large distance and the process of rebound to be distorted. Comparison to the experiment data has revealed that the process of rebound takes place with front wheels blocked. Consequently, the condition involving the value determined according to the limit value for tire to dry asphalt friction with the front wheels blocked has been introduced into the model. A system of four equations is used to calculate the model

$$\begin{cases} m_1 \ddot{x}_1 + k_1 \dot{x}_1 + c_1 x_1 + k_2 (\dot{x}_1 - \dot{x}_2) + c_2 (x_1 - x_2) = 0; \\ m_2 \ddot{x}_2 + k_2 (\dot{x}_2 - \dot{x}_1) + c_2 (x_2 - x_1) + k_3 (\dot{x}_2 - \dot{x}_3) + c_3 (x_2 - x_3) = 0; \\ m_3 \ddot{x}_3 + k_3 (\dot{x}_3 - \dot{x}_2) + c_3 (x_3 - x_2) + k_4 (\dot{x}_3 - \dot{x}_4) + c_4 (x_3 - x_4) = F \mu_3; \\ m_4 \ddot{x}_4 + k_4 (\dot{x}_4 - \dot{x}_3) + c_4 (x_4 - x_3) + k_5 (\dot{x}_4 - \dot{x}_5) + c_5 (x_4 - x_5) = 0; \end{cases} \quad (6)$$

where $F = m_f g$, m_f – vehicle mass imposed on the front suspension, and μ_3 – dry asphalt friction with the front wheel.

To identify the vital parameters, the fourth equation is used to reflect its links to the vehicle body. c_4 and k_4 are the general characteristics of the seat belt and thoracic cell, respectively. This is the contacting link between the occupant and the vehicle body during the impact. c_5 and k_5 are the general characteristics of the backrest and occupant's back, respectively. This model also implies three crumple zones.

Zone 1: requirements to this zone have already been described in the three-mass model. Nonetheless, the present model is calculated for a different distribution of the masses (Table 1, column on the right). In the three-mass model, all occupants' masses are included into the vehicle body mass. Moreover, in the three-mass model, all masses of the fender and other unspecified elements of the front crumple zone are attributed to the vehicle body mass. In this case, the mass of this zone is added to mass m_2 , which also includes the masses of the aforementioned units. With the bumper stiffness assumed to be 420 kN/m, bumper displacement and deformation have been determined (Fig. 10). The graph suggests that, as soon as the initial deformation speed of 8 km/h is exceeded, plastic deformation of bumper starts and becomes stabilized as soon as 11 km/h initial deformation speed is reached.

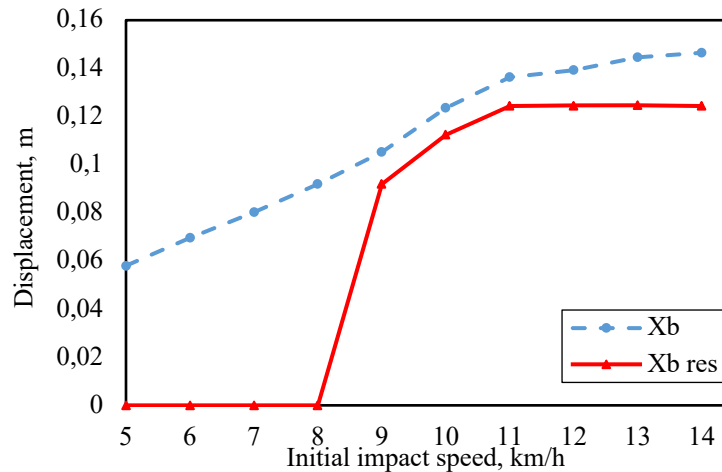


Fig. 10. Dependence of bumper displacement (X_b) and residual deformation ($X_b \text{ res}$) on the initial impact speed

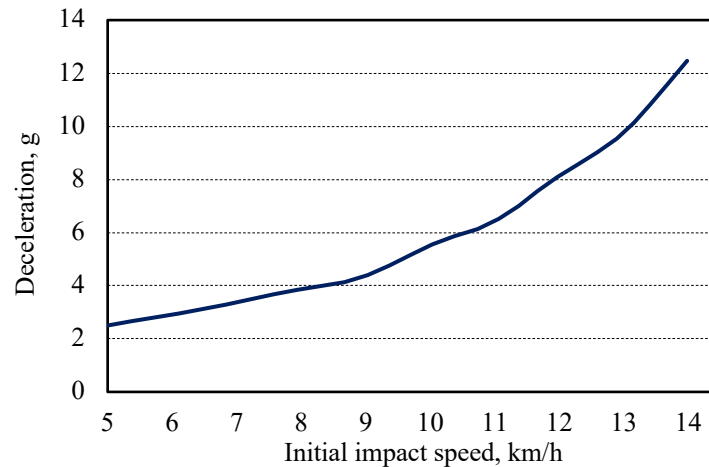


Fig. 11. Dependence of the vehicle body deceleration on the initial impact speed

The effect of the bumper crumple zone on the vehicle body deceleration is presented in Fig. 11. Vehicle body deceleration may be noticed to not exceed 4 g (the condition mentioned above) at the initial impact speed of 8 km/h. Moreover, as soon as bumper deformation has started, vehicle body deceleration temporarily stabilizes. This indicates that, as the bumper is deforming, a share of the impact energy is absorbed additionally (taking into account absorption of energy of the bumper dampers). After the bumper has deformed, vehicle body deceleration increases remarkably. Characteristics for other zones have been selected in line with the principle stating that plastic deformation of the subsequent zone starts only after the preceding zone has been deformed, and the zone deformation selected is as close as possible to the limit posing hazard to the occupant (to make the maximum possible use of the zone energy absorption).

Zone 2: mass 2 reflecting the zone in the model accounts for almost the entire front part of the vehicle (engine zone). Side member (its front part to the engine) has the greatest effect on the dynamic characteristics of this zone. The zone shall meet the following requirement: in case of a head-on collision at the speed of up to 50 km/h, the zone has to be deformed, i.e. to have absorbed the energy to the maximum, while zone 3 has to remain undamaged. Displacement and deformation of zone 2 are presented in Fig. 12.

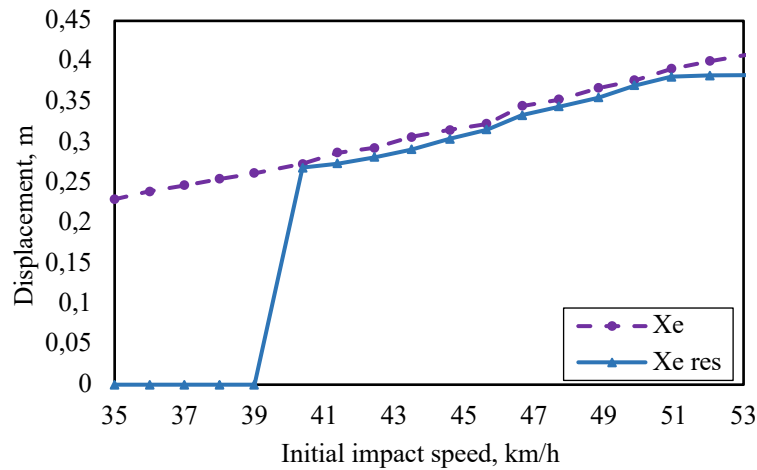


Fig. 12. Dependence of vehicle 2 zone displacement (X_e) and residual deformation ($X_{e\ res}$) on the initial impact speed

Engine zone mass and dimensions are considerably larger compared with those of the bumper; hence, deformation of the former lasts for a longer period of time. It starts as soon as the initial impact speed starts exceeding 39 km/h and ends at 49 km/h. A hike may be observed when analyzing the thoracic cell deceleration in the course of this deformation (Fig. 13). As soon as deformation of this zone has started, deceleration drops, i.e. the engine zone absorbs a share of the impact energy during its deformation, and the deceleration increases slower during deformation. Deceleration starts increasing faster as soon as the initial impact speed limit of 49 km/h is exceeded.

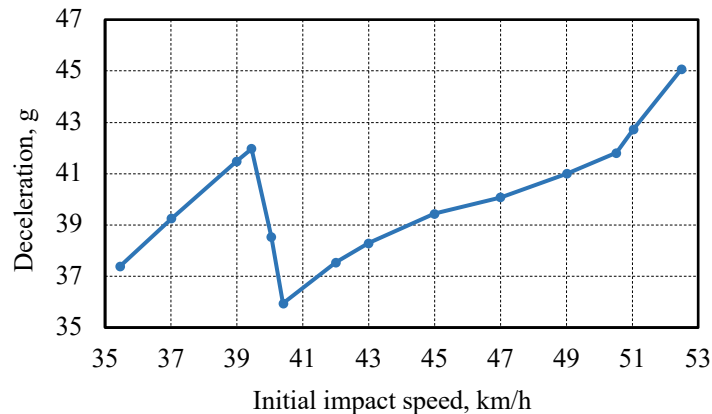


Fig. 13. Dependence of thoracic cell deceleration on the initial impact speed

Zone 3: the zone includes the vehicle body and the part of the side member behind the engine. The key elements resisting the impact and absorbing the energy are the part of the side member and the front wall of the passenger compartment. It should be noted that, at the control collision speed (64 km/h), the permissible deceleration for an occupant shall not be exceeded. In this model (Fig. 9), an occupant is considered as a single mass, and, as chest movement is controlled by the vehicle safety systems, it is assumed to be reflected by the movement of mass m_4 . According to the general requirements specified above, maximum deceleration of chest shall not exceed 60 g at the control speed. This is the only requirement applying to this zone, but it is key during the vehicle impact. The whole process of deformation is presented in Fig. 14. Deformation of the longitudinal member behind the engine starts at the initial impact speed of 57 km/h. As soon as 74 km/h is reached, deformation of the longitudinal member and front wall is completed. This is where the final crumple zone is defined.

As the initial impact speed is increasing, the impact energy is absorbed by the remaining vehicle body (containing the occupants as well) and by the occupants' safety systems.

The data provided in Fig. 14 suggest that the residual deformation is greater than the displacement. The missing share of the displacement is replaced by additional deformation of the zones discussed above. Stiffness of the model elements is assumed to be linearly variable and reaches ten times higher values compared with the initial ones as the residual deformation of masses is ending. As soon as the loads have increased considerably (50 km/h of the initial impact speed have been exceeded), the zones are subject to additional deformation to compensate for the vehicle body displacement (Fig. 14). In this zone (and all the safety tests), the most important is to not exceed the permissible deceleration (in this case – 60 g for thoracic cell) at the initial impact speed of 64 km/h (Fig. 15).

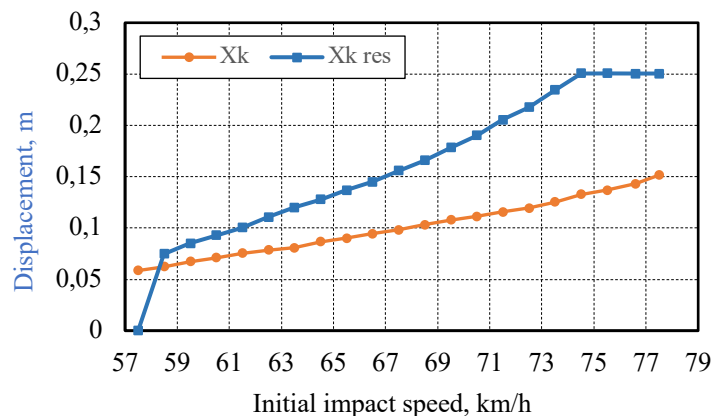


Fig. 14. Dependence of vehicle body displacement (X_k) and residual deformations ($X_k \text{ res}$) on the speed

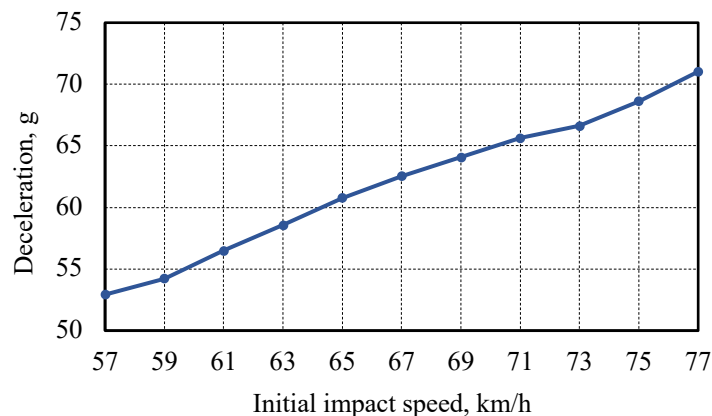


Fig. 15. Dependence of thoracic cell deceleration on the initial impact speed

Application of the four-mass model has involved revision of the damping effect on the impact process as well. The simulation results are presented in Fig. 16. Values k/k_{\max} from 0 to 1 correspond to variation of the damping coefficient for the bumper zone, 1.2 to 2 — engine zone, and 2.2 to 3 — vehicle body zone. Although increase in damping of the bumper zone reduces the deceleration acting on the occupant, the consequences of variation in damping of zone 2 are inconclusive. Fig. 17a, b presents the dependences of deceleration of individual masses when the impact takes place at 64 km/h. It could be observed that adjustment of the damping coefficient for zone 2 leads to changes in the excitation frequencies of the engine and vehicle body, increase of the amplitudes, and the deceleration acting on the occupant may increase as well. This explains the trend which could be observed in contemporary structures, where additional damping elements (gas or fluid) are used only in the bumper zone, and the engine zone is fitted only with porous plastic fillers characterized by lower

damping coefficient. As the damping coefficient for zone 3 is being increased, the deceleration for thoracic cell is increasing as well. The results suggest that the number of occupants in the light passenger vehicle also influences the impact process.

Hence, the deformation elements, damping installations for zones 2 and 3, should be designed only following careful consideration of all potential options. The four-mass model also enables verification of the structure of the backrest or identification of the specifications for its design.

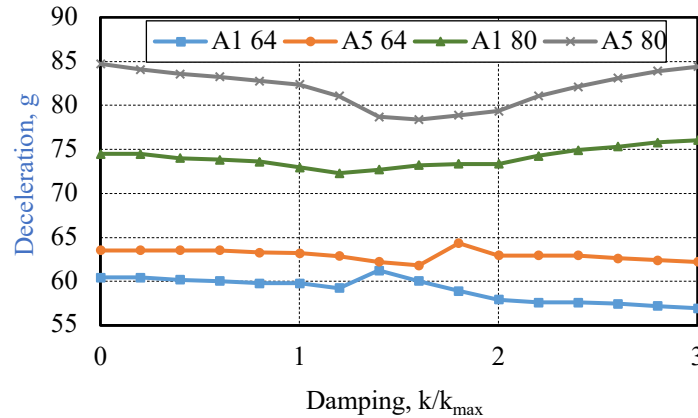


Fig. 16. Dependence of deceleration values in case of the impact at 64 and 80 km/h on the damping; where A1 and A5 – respectively, one and five occupants

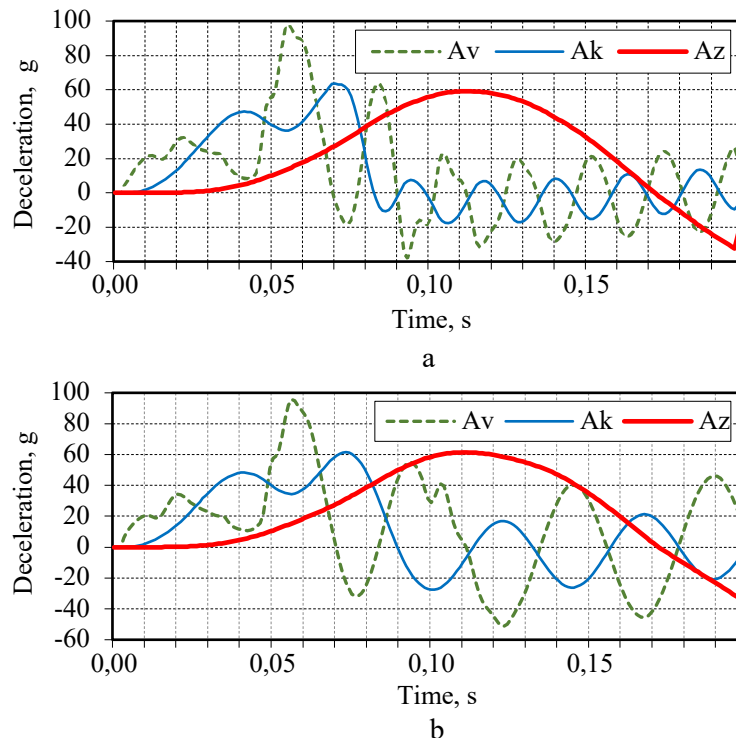


Fig. 17. Dependence of deceleration of vehicle engine zone (A_v), vehicle body (A_k), occupant's body (A_z) in case of an impact at the speed of 64 km/h, where the damping coefficients for zone 2: a - 1.3, b - 2.6.

Fig. 18a, b presents the dependence of the speed of occupant's frame at the 64 km/h impact (the seat belts are elastic). The occupant's speeds could be noticed to considerably increase those of the vehicle body throughout the impact, and the occupant is thrust into the backrest at the speed similar to that at the initial stage of impact. Although the speed of the vehicle body is not high at that moment, this stage may be more hazardous than the stage of forward movement. This issue is not analysed

further in more details owing to a more accurate occupant's model required, as it is not the thoracic cell or vertebrae which are the determining factor but deceleration of the head and forces acting on the neck.

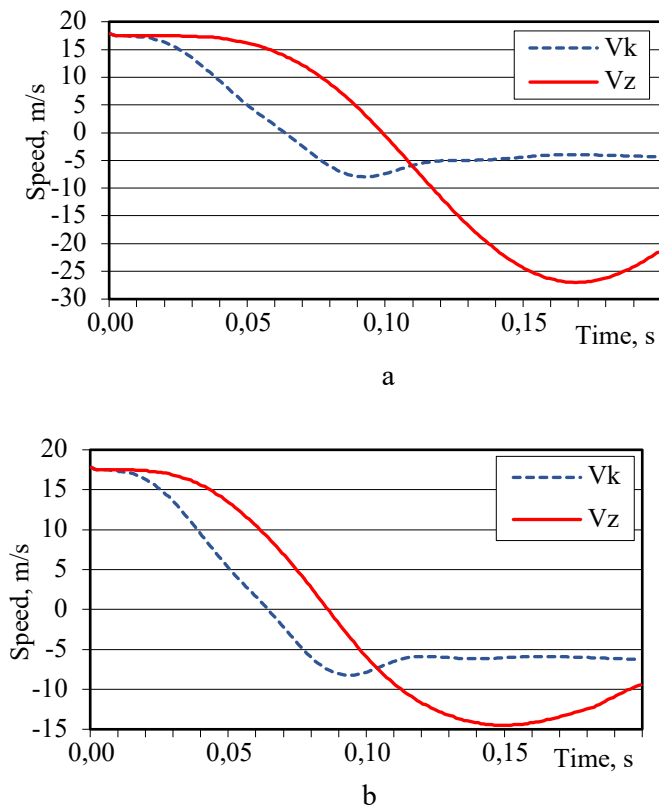


Fig. 18. Dependence of occupant's body (V_z) and vehicle body (V_k) speed in case of the impact at the speed of 64 km/h: a – without the safety system damping, b – with the safety system damping

The results suggest that the model is fairly comprehensive in terms of representation of the impact process and the processes taking place. Accuracy of the dynamic parameters of the units used has considerable effect on the accuracy of the results. They obviously cannot be described very accurately, and simplification is required. Dynamic characteristics of the units have been assumed to not change over time, and maximum displacement of individual units to be limited.

5. CONCLUSIONS

1. Simple models of the front crumple zone of the vehicle have been analyzed; the limits for the key parameters (damping and stiffness coefficient) for the deformable elements in these zones have been identified; and the methodology for determination of the parameters has been revised for specific vehicles. Key determining factors have been identified.
2. The damping elements in all the zones reduce the maximum values of the rebound speed, deceleration, and deformation, but should be used carefully in zones 2 and 3, as highly effective dampers lead to changes in the characteristic frequencies of the zones, and the thoracic cell deceleration values might increase. Although human mass is not large compared to that of a vehicle body, the number of occupants within the passenger compartment influences the impact process, in particular, the emerging sweeps, which makes optimization of the deformable elements of the zones more difficult.

3. The four-mass model enables assessing the influence of not only seat belts, but also backrests, which, however, requires a more complex occupant model. In the four-mass model, occupant's loads provide sufficient preconditions for further optimization of the crumple zones.

References

1. *Official Journal of the European Communities*. Directive 96/79/EC of the European Parliament and of the Council of 16 December 1996 on the protection of occupants of motor vehicles in the event of a frontal impact and amending Directive 70/156/EEC. 1997. Vol. 40. 50 p.
2. Рябчинский, А.И. *Пассивная безопасность автомобиля*. Москва. Машиностроение. 1983. 145 с. [In Russian: Ryabchinsky, A.I. *Passive car safety*. Moscow. Mashinostrojenije. 1983. 145 p.].
3. Афанасьев, Л.Л. & Дьяков, А.Б. & Иларионов, В.А. *Конструктивная безопасность автомобиля*. Москва. Машиностроение. 1983. 212с. [In Russian Afanasyev, L.L. & Dyakov, A.B. & Parionov, V.A. *Structural car safety*. Moscow. Mashinostrojenije. 1983. 212 p.].
4. Deb, A. & Biswas, U. & Chou, C. HIC(d) and Its Relation with Headform Rotational Acceleration in Vehicle Upper Interior Head Impact Safety Assessment. *SAE Int. J. Passeng. Cars - Mech. Syst.* 2009. Vol. 1(1). P. 142-149. DOI: 10.4271/2008-01-0186.
5. Yamaguchi, S. & Taneda, K. Current Status of Correlation Between CTP and FST. *Proc. of the 13th Inter. Technical Confer. on Experimental Safety Vehicles*. Paris, France. November 4-7, 1991. 720 p.
6. Wicher, J. *Bezpieczeństwo samochodów i ruchu drogowego*. [In Polish: *Car and road traffic safety*]. Warsaw. WKiŁ. 2002. 276 p.
7. Seiffert, U. & Wech, L. *Automotive Safety Handbook*. Warrendale, SAE International. 2007. 306 p.
8. Fenton, J. 1998. *Handbook of Automotive Body Construction and Design Analysis*. London, Professional Engineering Publishing. 455 p. Huang, Matthew. 2002. *Vehicle crash mechanics*. CRC press, 481 p.
9. Executive Cars Crash Test Results. 1998. *The European Bureau of the Alliance Internationale de Tourisme & Federation de L'Automobile*. Brussels, Euro NCAP September. 28p.
10. Huang, M. *Vehicle crash mechanics*. CRS press. 2002. 481 p.
11. Pahlavani, M. & Marzbanrad, J. Crashworthiness study of a full vehicle-lumped model using parameters optimisation. *International Journal of Crashworthiness*. 2015. Vol 20. No 6. P. 573-591. DOI: 10.1080/13588265.2015.1068910.
12. Ofochebe, S.M. & Ozoegwu, C.G. & Enibe, S.O. Performance evaluation of vehicle front structure in crash energy management using lumped mass spring system. *Advanced Modeling and Simulation in Engineering Sciences*. 2015. Vol. 2. No 1. P. 2. DOI: 10.1186/s40323-015-0020-1.
13. Pawlus, W. & Reza, K.H. & Robbersmyr, K. Development of lumped-parameter mathematical models for a vehicle localized impact. *Journal of Mechanical Science and Technology*. 2011. Vol. 25. P. 1737-1747. DOI: 10.1007/s12206-011-0505-x.
14. Munyazikwiye, B. *Optimization of Vehicle-to-Vehicle Frontal Crash Model Based on Measured Data Using Genetic Algorithm*. IEEE Access. 2017. Vol. 5. P. 3131-3138.
15. Wierzbicki, T. & Abramowicz, W. On the crushing mechanics of thin-walled structures. *Journal of Applied Mechanics*. 1983. Vol. 50. P. 727-734. DOI: 10.1115/1.3167137.
16. Lawrence, G.J.L., etc. Bonnet Leading Edge Sub-Systems Test for Cars to Assess. *Proc. for the 13th Inter. Technical Confer. on Experimental Safety Vehicles*. Paris. France. November 4-7, 1991. 720 p.